THE JOURNAL OF PHYSICAL CHEMISTRY LETTERS
A JOURNAL OF THE AMERICAN CHEMICAL SOCIETY

pubs.acs.org/JPCL

Letter

Nonradiative Dynamics Induced by Vacancies in Wide-Gap III-Nitrides: Ab Initio Time-Domain Analysis

Yuxin Yang, Zhiming Shi,* Shoufeng Zhang, Xiaobao Ma, Jiangxiao Bai, Dashuo Fan, Hang Zang, Xiaojuan Sun,* and Dabing Li*

Cite This: *J. Phys. Chem. Lett.* 2023, 14, 6719−6725

Read Online

ACCESS | Metrics & More | Article Recommendations | Supporting Information

ABSTRACT: Insightful understanding of defect properties and prevention of defect damage are among the biggest issues in the development of photoelectronic devices based on wide-gap III-nitride semiconductors. Here, we have investigated the vacancy-induced carrier nonradiative dynamics in wide-gap III-nitrides (GaN, AlN, and $Al_xGa_{1-x}N$) by ab initio molecular dynamics and nonadiabatic (NA) quantum dynamics simulations since the considerable defect density in epitaxy samples. E-h recombination is hardly affected by V_{cation}, which created shallow states near the VBM. Our findings demonstrate that V_N in AlN creates defect-assisted nonradiative recombination centers and shortens the recombination time (τ) as in the Shockley-Read-Hall (SRH) model. In GaN, V_N improves the NA coupling between the CBM and the VBM. Additionally, increasing x in the $Al_xGa_{1-x}N$ alloys accelerates nonradiative recombination, which may be an important issue in further improving the IQE of high Al-content $Al_xGa_{1-x}N$ alloys. These findings have significant implications for the improvement of wide-gap III-nitrides-based photoelectronic devices.

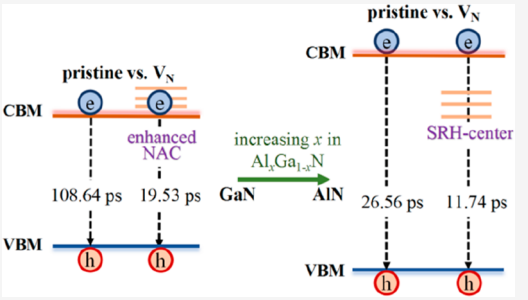

The wide-gap III-nitrides (AlN and GaN) as a new generation of semiconductors are promising materials for high-power,[1] power-switching,[2] and photoelectronic[3] devices owing to their outstanding characteristics, namely their wide bandgap, high breakdown field,[4] high saturation velocity,[5] and excellent chemical and thermal stability.[6] Due to the lack of natural substrates, the high-density defects, including point defects and dislocations, introduced during material growth hinder the efficiency and reliability of devices.[7−9] These defects lead to complaints as the nonradiative recombination[10−12] and current leakage centers,[13,14] which reduce the gain and increase the noise in particular photoelectronic devices.[10,12,13] This problem is more serious in high Al content $Al_xGa_{1-x}N$ alloys. Because the density of defects magnifies as Al content increases, this results in the reduction of the internal quantum efficiency (IQE)[15,16] and further reduction of the external quantum efficiency (EQE).[13,14,17−21] For instance, Lu J et al.[15] reported that upon comparing different samples, the peak IQE reduced from 73% to 56% as the Al content increased from 22% to 54%. Therefore, it becomes critical to understand the underlying mechanism and then minimize the impact of defects detrimental to the performance of the relative devices.

Many efforts have been donated to study the dislocation[22−24] and have demonstrated that they are nonradiative recombination centers and thus poisoned the luminescence efficiency.[10−12] With the great improvements that have been achieved in the preparation technique, the dislocation density can be reduced to 10^7 cm^{-2} or lower in GaN epilayer,[25,26] which has less impact on the efficiency. The experimental understanding and identification of point defects remain controversial despite considerable progress in GaN-based photoelectronic devices over the last few decades. However, it is also unignorable. First-principles calculations have been successful in the research of point defect properties in GaN-based semiconductors. Previous reports indicated that vacancies are the most relevant defects due to their high densities in samples.[27−30] Nitrogen vacancies (V_N) showed lower formation energy than other point defects in GaN[31,32] but sharply decline as Al content increased.[33] The yellow band in GaN was attributed to the gallium vacancies (V_{Ga}).[34] Aluminum vacancies (V_{Al}) also cause defect luminescence.[35] Most studies mainly focused on the ground state of III-nitrides.[29−33] The characteristics of defects in excited states, particularly point defects involvement in the photon-to-electron power conversion, still need to be better understood.

Herein, we investigate the nonradiative recombination processes due to native point defects in GaN and AlN using state-of-the-art ab initio nonadiabatic molecular dynamics (NAMD) combined with real-time time-dependent density functional theory. Whether the defects introduce shallow or

Received: June 1, 2023
Accepted: July 14, 2023
Published: July 20, 2023

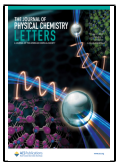

https://doi.org/10.1021/acs.jpclett.3c01515
J. Phys. Chem. Lett. 2023, 14, 6719−6725

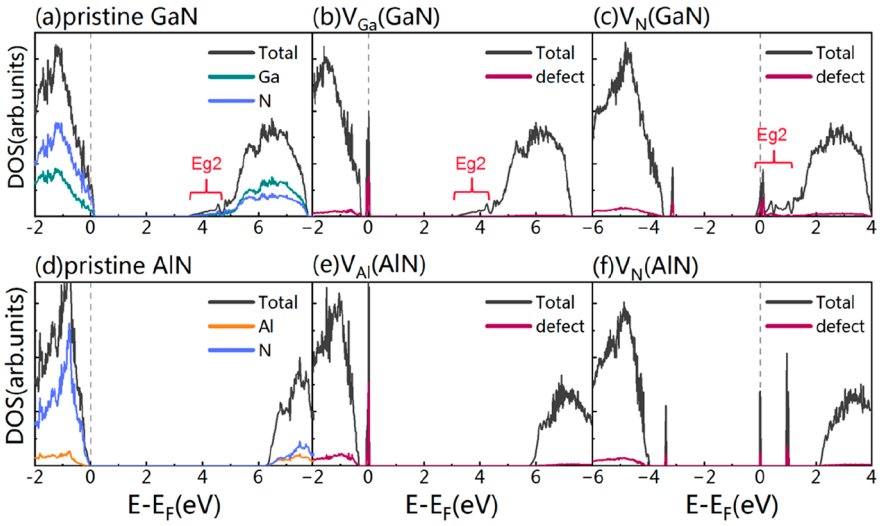

Figure 1. Atom-projected DOS for different defective and pristine GaN and AlN. (a–f) Pristine and defective GaN and AlN. The Fermi levels are set to zero and marked by dashed gray lines.

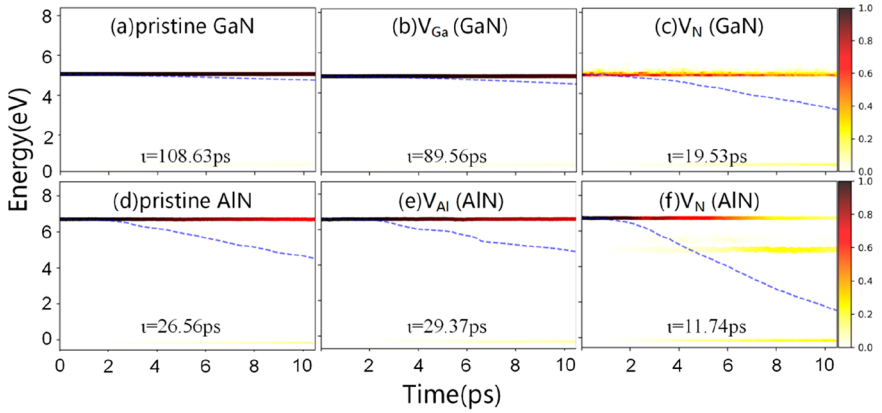

Figure 2. Time evolution of the average electron energy for pristine and defective GaN and AlN systems, with the colored bar indicating the electron population. The recombination time (τ) was marked.

deep trap states inside the fundamental band gap, the charge recombination in defective GaN is significantly slower than that in defective AlN. The properties of cation vacancies (V_{cation}) in AlN and GaN are fully occupied defects and have little effect on carrier recombination. However, the V_N accelerates the nonradiative recombination in both GaN and AlN. There is a vast difference in that the defect state of V_N in GaN does not locate in the bandgap while the defect state of V_N in AlN forms defect-assisted nonradiative-recombination centers. Different mechanisms for the acceleration of nonradiative recombination are revealed. It may explain why GaN usually exhibits better IQE than AlN and $Al_xGa_{1-x}N$ alloys.[15,16] Meanwhile, we investigate the impact of charge states and Al contents on carrier nonradiative recombination. We believe that our results are valuable for further improving the efficiency of photoelectronic devices based on wide-gap III-nitrides.

Methods. The geometry optimization, electronic structure, and adiabatic molecular dynamics trajectories are performed using the Vienna Ab initio Simulation Package (VASP).[36] The projector augmented wave (PAW)[37] method is employed to describe electron–ion interaction, and the Perdew–Burke–Ernzerhof (PBE) functional under the generalized gradient approximation (GGA).[38] The NAMD simulations are carried out by the Hefei-NAMD code,[39] employing the classical path approximation within the TDKS.[40] This method has been proven to be reliable in a variety of materials.[41−47] The ion cores are treated classically due to their heavier and slower nature than electrons, while the electrons are described quantum mechanically with real-time time-dependent density functional theory.[48,49] The nonadiabatic couplings (NACs) are calculated using the CA-NAC package.[50−52] More details can be seen in the Supporting Information.

The density of states (DOS) for vacancies in GaN and AlN is shown in Figure 1, and the results for pristine GaN and AlN are also provided. As reported, the valence band maximum (VBM) and conduction band minimum (CBM) are contributed by the *p*-orbital and *s*-orbital of N atoms for both GaN and AlN.[53,54] The distinction between GaN and AlN near the CBM can be observed, where is a quasi-bandgap (named Eg2 by Chris G. van der Walle et al.[30]) in GaN, but disappeared in AlN, as shown in Figures 1a and d. We considered both cation (Ga or Al) and anion (N) vacancies. The cation vacancy introduces a shallow 4-fold-degenerate defect state near the VBM, thus exhibiting acceptor-type properties in both GaN and AlN, as shown in Figures 1b and e. The cases for N vacancies are different. The dangling cations induce one occupied defective state and three unoccupied defective states located near the VBM and CBM, respectively (Figure 1c),

https://doi.org/10.1021/acs.jpclett.3c01515
J. Phys. Chem. Lett. 2023, 14, 6719−6725

Table 1. Electron-Hole Recombination Time Obtained by Fitting: Canonically Averaged Absolute Values of NAC between Pairs of the VBM and CBM for Different Systems

	GaN			AlN		
	pristine	V_{Ga}	V_N	pristine	V_{Al}	V_N
Recombination time (ps)	108.64	89.56	19.53	26.56	29.37	11.74
$NAC_{VBM-CBM}$ (meV)	0.18	0.23	0.76	0.30	0.28	1.27

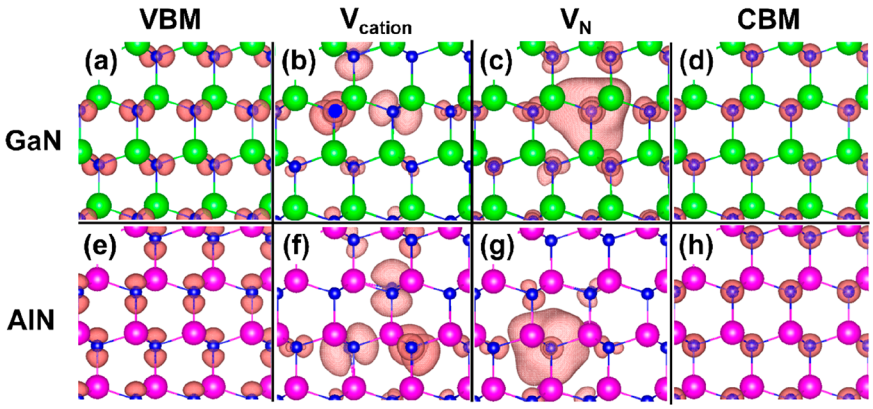

Figure 3. Spatial distribution of wave functions for (a, e) VBM, (d, h) CBM, and defect states of (b, c) GaN and (f, g) AlN. The isosurface is set to 1.5×10^{-3} e/Å^{-3}.

indicating the inequivalence of the four dangling bonds. It is noteworthy that the defect states inside the Eg2 form deep states in AlN but shallow ones in GaN. Upon heating to 300 K, time-dependent energy evolution of the VBM, the CBM, and the defect states for GaN and AlN can be seen in Figure S2.

Figure 2 depicts the time-dependent e-h recombination process of the electron. More details can be found in Figure S3. The recombination time (τ) for the CBM population decay was obtained by fitting the decay curve to the exponential function $\exp(-t/\tau)$ with a first-order linear expansion as previously reported.[55,56] The recombination time in pristine GaN, which is 108.63 ps (Figure 2a), is considerably slower than that in pristine AlN, which is 26.56 ps (Figure 2d) . The V_{cation} has little influence on the recombination process, causing V_{Ga} to slightly accelerate to 89.56 ps (Figure 2b) and V_{Al} to somewhat slow down to 29.37 ps (Figure 2e). The V_N considerably speeds up the recombination in both GaN and AlN via different mechanisms. In the GaN, the defect states are in the Eg2 above the CBM. The acceleration is attributed to the enhanced el-ph coupling between defects, CBM, and VBM. In the AlN, deep defect states located inside the bandgap formed a nonradiative recombination center and trapped the hot electrons (the yellow state in Figure 2f) which is consistent with the SRH mechanism.

We can also understand these results by calculating the nonadiabatic coupling (NAC) between the donor and acceptor states. Generally, a stronger NAC leads to faster e-h recombination. We list the NAC between the VBM and CBM ($NAC_{VBM-CBM}$) in Table 1 to quantify the coupling strength of the system. As references, the $NAC_{VBM-CBM}$ are 0.18 and 0.30 meV for pristine GaN and AlN, respectively. The V_{cation} has little impact on $NAC_{VBM-CBM}$, 0.23 meV for V_{Ga} and 0.28 meV for V_{Al}. As a result, the τ of V_{cation} is comparable to that of pristine materials. On the other hand, the $NAC_{VBM-CBM}$ of V_N is 0.76 meV in GaN and 1.27 meV in AlN, which is almost four times longer than those in pristine materials. The strengthened el-ph coupling induced by V_N shortens τ sharply. However, the mechanisms are different for GaN and AlN. The NACs between defect states, the VBM, and the CBM are shown in Figure S4. In contrast to AlN (Figures S4c,d), GaN exhibits significant NACs between the CBM and V_N states (VBM+3 and VBM+4). As a result, the V_N states facilitate defect-assisted nonradiative-recombination centers in AlN but just improve the el-ph coupling in GaN. We calculated the e-h recombination of pristine GaN, V_{Ga}, and V_N (GaN) at different temperatures (200, 300, and 400 K) as shown in Figure S5, with the increase of temperature, the adiabatic coupling is enhanced, and the e-h recombination becomes faster.

The overlap between the related wave functions also serves to justify the strength of the NAC between the defect states and the frontier orbitals. We extract a structure from the MD trajectory and plot the spatial distribution of wave functions $|\varphi|^2$ for the frontier and defect orbitals in Figure 3, consistent with the DOS in Figure 1. For the pristine systems, in agreement with previous investigations,[57] the VBM and CBM are distributed mainly on the N-*2p* (Figures 3a and e) and N-*2s* (Figures 3d and h) orbitals, respectively. The wave functions of V_{Ga} and V_{Al} strongly overlap with VBM (Figures 3b and f), indicating the strong coupling between them. However, the overlap between V_{cation} and CBM is quite weak, so the V_{cation} exhibits little impact on electron dynamics for both GaN and AlN. The wave function of V_N considerably overlaps with CBM in GaN (Figure 3c), but not in AlN (Figure 3g), indicating that the V_N induces stronger el-ph coupling in GaN than that in AlN. This is the reason that the V_N shows larger NACs between defect states and CBM in GaN. Again, it confirmed that the acceleration of e-h nonradiative recombination is induced by stronger el-ph coupling in GaN and by supporting defect-assisted nonradiative recombination centers.

To comprehend the mechanism of charge carrier dynamics influenced by defects, we calculated Fourier transforms (FTs) of the energy fluctuations. Here, the vibrational modes that cause energy loss as heat and improve nonradiative charge carrier recombination were discovered by learning the phonon modes directly participating in the dynamic process from the FTs spectra. We presented the spectra of FTs in pristine and

https://doi.org/10.1021/acs.jpclett.3c01515
J. Phys. Chem. Lett. 2023, 14, 6719−6725

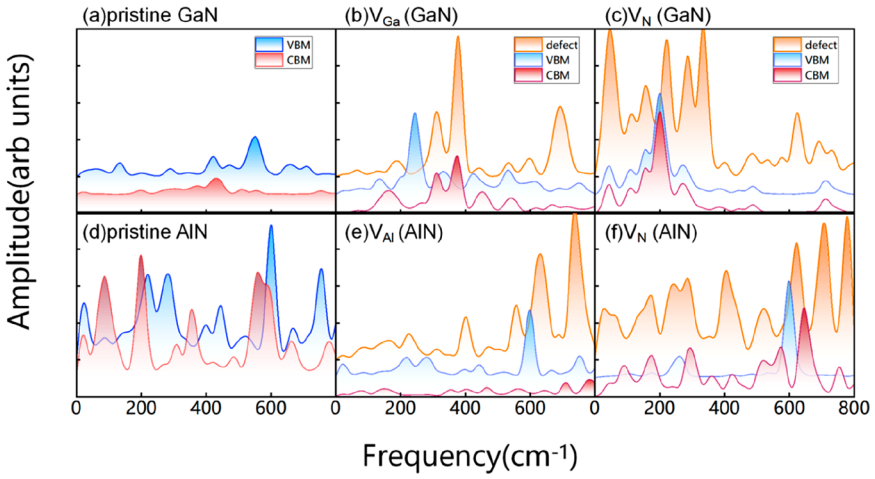

Figure 4. Fourier transform (FT) spectra of the phonon-induced fluctuations of the VBM, CBM, and defect energy levels in the GaN and AlN systems for (a) pristine GaN, (b) pristine AlN, (c) V_{Ga}, (d) V_{Al}, (e) V_N in GaN, and (f) V_N in AlN.

Table 2. Electron-Hole Recombination Time Obtained by Fitting: Canonically Averaged Absolute Values of NAC between the VBM and CBM for Different Charge Defects

	GaN			AlN		
	V_{Ga}^{-3}	V_N^{+1}	V_N^{+3}	V_{Al}^{-3}	V_N^{+1}	V_N^{+3}
Recombination time (ps)	77.20	11.45	16.46	25.27	12.79	11.03
$NAC_{VBM-CBM}$ (meV)	0.28	0.87	0.79	0.31	1.24	1.31

defective systems in Figure 4. For pristine GaN, the e-h recombination was driven by the 555.94 cm^{-1} phonon mode (Figure 4a), which corresponds to the E_1(TO) mode.[58] As for the defective states, the symmetry is broken. Such perturbation (or phonon scattering) can introduce many more new phonon modes. Compared with the pristine GaN, the contribution of defects in V_{Ga} is mainly located in 364.61 cm^{-1}, 378.04 cm^{-1}, and 694.76 cm^{-1}, and the occurrence of high-frequency vibration mode means that the core velocity is higher (Figures 4a and b). Since these higher-frequency phonon modes are associated with the large nuclear velocities, and the resulting NAC is big, as follows from eq 1 in the SI. The same trend was also observed in AlN. For the V_N systems, the defect states of V_N couples with the lower phonons at 0−400 cm^{-1} and a common peak at 200.14 cm^{-1} in GaN (Figure 4c), but with higher phonons at 533.71 and 711.60 cm^{-1} in AlN (Figure 4f) than those in pristine systems. In general, the above analysis indicates that defects contributed prominently to el-ph coupling.

Besides the neutral state, the vacancies are always charged in GaN and AlN, as demonstrated by both theoretical and experimental works.[28,30,59−61] We also studied the effect of charged states on e-h recombination for vacancies. The stable charge states were adapted from previous reports.[30,33] Considering the formation energy, the −3 charged state was selected for cationic vacancies (V_{cation}^{-3}), +1 and +3 charge states for anionic vacancies (V_N^{+1} and V_N^{+3}). The V_{cation} was a fully occupied defect with a negative charge defect that repels electrons, as is shown in Figure S6a,d. It has a negligible effect on electron evolution, which in turn causes an insignificant effect on e-h recombination, as depicted in Figure S7 and Table 2.

The charged V_N demonstrated distinct characteristics in the AlN and GaN. In the AlN, the defect states go deeper but the τ just changed little when the charge states increase from 0 to +3 as shown in Figure S6e,f and Table 2. For the GaN, the defect states of V_N^{+1} located in the Eg2 shift toward the CBM by comparing with that of neutral states and almost overlap with the CBM, resulting in the τ considerably reduced due to the enhanced coupling between defect states and CBM, as shown in Table 2. As increasing positive charge to +3, the defect states keep shifting into the bandgap and forming the shallow defect states below CBM by ∼1.3 eV, as shown in Figure S6c. The results of the NAC calculation in charge systems with in Figure S8 and FTs spectra in Figure S9 support the change of evolution speed, and the value is $V_N^{+1} > V_N^{+3} > V_N^0$. In Figure 5a, there are two stages in the evolution process for the V_N^{+3} both in GaN and AlN. First, the excited electrons on the CBM are rapidly trapped by the shallow defect states and then slowly relax toward the VBM. As for V_N^{+1}, the defect state has a smaller probability of being occupied by electron but greatly contributes to the nonradiative recombination rate. We also calculated V_N^{-1} in AlN since the stability was confirmed previously. The properties are shown in Figure S10 and the evolution is not different from that of other V_N (AlN) systems. Because V_N in GaN is the most sensitive to charge states among all of the defective systems, it is feasible to reduce the nonradiative recombination by tuning the Fermi-level to obtain the desirable charge states for V_N. Since the different charge states of V_N in AlN have little effect on the nonradiative recombination, it may be useless in AlN.

Alloying is an effective route for engineering the photoelectronic properties of III-nitrides and has achieved great industrial success, such as $In_xGa_{1-x}N$ and $Al_xGa_{1-x}N$.[18,62,63] Does the nonradiative recombination induced by vacancies also have the potential to be tuned by alloying? To this end, we have studied the electronic nonradiative dynamics of V_N in $Al_xGa_{1-x}N$ alloys with x of 0.25, 0.50, and 0.75 because the V_{cation} showed similar nonradiative behavior in GaN and AlN. The results are displayed in Figure 5c and d. With increasing x

https://doi.org/10.1021/acs.jpclett.3c01515
J. Phys. Chem. Lett. 2023, 14, 6719−6725

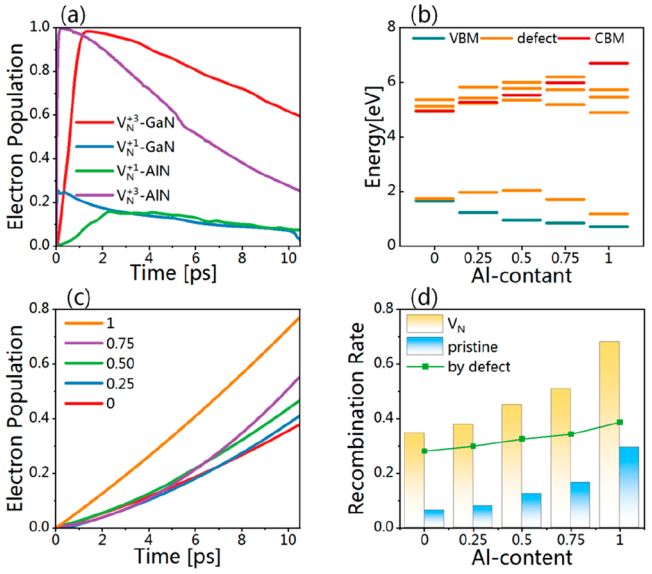

Figure 5. (a) The electron population of the defect states in the e-h recombination dynamics process in V_N^{+1}(GaN), V_N^{+1}(AlN), V_N^{+3}(GaN), V_N^{+3}(AlN). (b) Energy levels of CBM (red line), VBM (blue line), and defect states (orange line) of the V_N systems in different Al-content $Al_xGa_{1-x}N$ as 0, 0.25, 0.50, 0.75, and 1 for the average configuration at 300 K. (c) The electron population of the VBM in the e-h recombination dynamics process in the different Al-content V_N systems. (d) e-h recombined percentage for different systems of V_N and pristine after 10 ps. The by-defect e-h recombined percentages are shown by green color bars.

in $Al_xGa_{1-x}N$ alloys, the V_N defect states gradually shifted from Eg2 to the band gap, as is shown in Figure 5b. As a result, the V_N strengthened the el-ph coupling for low Al content but formed nonradiative recombination centers for high Al content. The nonradiative recombination ratio increases within 10 ps indicating that the higher the Al content, the faster the nonradiative recombination in $Al_xGa_{1-x}N$ alloys as shown in Figure 5c and d. Consequently, the nonradiative recombination rate increased, and the internal quantum efficiency (IQE) was hindered by the increasing Al content in $Al_xGa_{1-x}N$ alloys, which was consistent with the previous reports.[15,17,19,64] Therefore, the different V_N-induced nonradiative dynamics are also crucial issues for the further improvement of relevant devices.

To summarize, using time-dependent ab initio NAMD simulation, we have investigated the e-h nonradiative recombination dynamics induced by vacancies in GaN and AlN. The V_{cation} formed shallow states near the VBM and hardly influenced the e-h recombination dynamics in both GaN and AlN. On the contrary, the V_N in both GaN and AlN considerably accelerates the e-h recombination by following different mechanism. Our analyses showed that the V_N states enhanced the el-ph coupling between the CBM, VBM and defect states in GaN but supported defect-assisted nonradiative recombination centers in AlN. The carrier nonradiative recombination can also be affected by the defect charge states. Furthermore, we find that the nonradiative recombination is accelerated by increasing the Al content in the $Al_xGa_{1-x}N$ alloy, which may be an unignorable factor of further improving the IQE of the high Al content $Al_xGa_{1-x}N$ alloy. These findings have important implications for the design of GaN-based optoelectronic conversion functional semiconductor materials.

■ ASSOCIATED CONTENT

Supporting Information

The Supporting Information is available free of charge at https://pubs.acs.org/doi/10.1021/acs.jpclett.3c01515.

Calculation details; Calculated band gap of GaN and AlN as a function of U(N); Time evolution of the eigenvalues for VBM, CBM, and defect states; The time evolution of the VBM, the CBM, and the defect state for GaN and AlN systems at 300 K; Additional figures and tables of e-h recombination properties; Time evolution of the average electron and hole energy for pristine GaN and AlN; Averaged absolute NACs between energy levels ranging from VBM to VBM+5 (CBM) for pristine, V_N, and V_{cation} for GaN and AlN systems, respectively; Pure dephasing times between pairs of the VBM, CBM, and defect states for different systems; Time dependent energy evolution for the pristine GaN,V_{Ga}, and V_N at 200, 300, and 400 K, respectively; Atom-projected DOS for different defective GaN and AlN systems with charge; Time evolution of the average electron and hole energy for different defective GaN and AlN systems with charge with the colored bar indicating the electron population; Averaged absolute NACs between energy levels ranging from VBM to VBM+5 for V_N and V_{cation} in GaN and AlN systems with charge, respectively; Fourier transform (FT) spectra of the phonon-induced fluctuations of the VBM, CBM, and defect energy levels in charged defect states in the GaN and AlN systems (PDF)

Transparent Peer Review report available (PDF)

■ AUTHOR INFORMATION

Corresponding Authors

Zhiming Shi − *State Key Laboratory of Luminescence and Applications, Changchun Institute of Optics, Fine Mechanics and Physics, Chinese Academy of Sciences, Changchun 130033, China;* orcid.org/0000-0002-1207-570X; Email: shizm@ciomp.ac.cn

Xiaojuan Sun − *State Key Laboratory of Luminescence and Applications, Changchun Institute of Optics, Fine Mechanics and Physics, Chinese Academy of Sciences, Changchun 130033, China;* orcid.org/0000-0001-6836-3893; Email: sunxj@ciomp.ac.cn

Dabing Li − *State Key Laboratory of Luminescence and Applications, Changchun Institute of Optics, Fine Mechanics and Physics, Chinese Academy of Sciences, Changchun 130033, China; Center of Materials Science and Optoelectronics Engineering, University of Chinese Academy of Sciences, Beijing 100049, China;* orcid.org/0000-0001-5353-1460; Email: lidb@ciomp.ac.cn

Authors

Yuxin Yang − *State Key Laboratory of Luminescence and Applications, Changchun Institute of Optics, Fine Mechanics and Physics, Chinese Academy of Sciences, Changchun 130033, China; Center of Materials Science and Optoelectronics Engineering, University of Chinese Academy of Sciences, Beijing 100049, China*

Shoufeng Zhang − *Department of Electronic Engineering, Guangxi University of Science and Technology, Liuzhou 545006, China;* orcid.org/0000-0001-6034-5041

https://doi.org/10.1021/acs.jpclett.3c01515
J. Phys. Chem. Lett. 2023, 14, 6719−6725

Xiaobao Ma − *State Key Laboratory of Luminescence and Applications, Changchun Institute of Optics, Fine Mechanics and Physics, Chinese Academy of Sciences, Changchun 130033, China; Center of Materials Science and Optoelectronics Engineering, University of Chinese Academy of Sciences, Beijing 100049, China*

Jiangxiao Bai − *State Key Laboratory of Luminescence and Applications, Changchun Institute of Optics, Fine Mechanics and Physics, Chinese Academy of Sciences, Changchun 130033, China; Center of Materials Science and Optoelectronics Engineering, University of Chinese Academy of Sciences, Beijing 100049, China*

Dashuo Fan − *State Key Laboratory of Luminescence and Applications, Changchun Institute of Optics, Fine Mechanics and Physics, Chinese Academy of Sciences, Changchun 130033, China; Center of Materials Science and Optoelectronics Engineering, University of Chinese Academy of Sciences, Beijing 100049, China*

Hang Zang − *State Key Laboratory of Luminescence and Applications, Changchun Institute of Optics, Fine Mechanics and Physics, Chinese Academy of Sciences, Changchun 130033, China;* orcid.org/0000-0002-1797-6857

Complete contact information is available at: https://pubs.acs.org/10.1021/acs.jpclett.3c01515

Notes

The authors declare no competing financial interest.

■ ACKNOWLEDGMENTS

The research reported in this publication was supported by the National Natural Science Foundation of China (12234018, 62121005, U21A201550, 61827813, 61834008) Key Research Program of Frontier Sciences, CAS (Grant No. ZDBS-LY-JSC026), the Youth Innovation Promotion Association of CAS (2019222), the CAS Talents Program and CAS Project for Young Scientists in Basic Research.

■ REFERENCES

(1) Wu, Y.-F.; Kapolnek, D.; Ibbetson, J. P.; Parikh, P.; Keller, B. P.; Mishra, U. K. Very-high power density AlGaN/GaN HEMTs. *IEEE T ELECTRON DEV* **2001**, *48*, 586−590.

(2) Ishida, M.; Ueda, T.; Tanaka, T.; Ueda, D. GaN on Si technologies for power switching devices. *IEEE T ELECTRON DEV* **2013**, *60*, 3053−3059.

(3) Akasaki, I.; Amano, H.; Kito, M.; Hiramatsu, K. Photoluminescence of Mg-doped p-type GaN and electroluminescence of GaN pn junction LED. *J. Lumin.* **1991**, *48*, 666−670.

(4) Saito, W.; Takada, Y.; Kuraguchi, M.; Tsuda, K.; Omura, I.; Ogura, T.; Ohashi, H. High breakdown voltage AlGaN-GaN power-HEMT design and high current density switching behavior. *IEEE T ELECTRON DEV* **2003**, *50*, 2528−2531.

(5) Ahi, K. Review of GaN-based devices for terahertz operation. *Opt. Eng.* **2017**, *56*, 090901−090901a.

(6) Liu, Q.; Lau, S. A review of the metal−GaN contact technology. *Solid-State Electron.* **1998**, *42*, 677−691.

(7) Meneghini, M.; Tazzoli, A.; Mura, G.; Meneghesso, G.; Zanoni, E. A review on the physical mechanisms that limit the reliability of GaN-based LEDs. *IEEE T ELECTRON DEV* **2010**, *57*, 108−118.

(8) Wang, Y.; Wang, X.; Zhu, B.; Shi, Z.; Yuan, J.; Gao, X.; Liu, Y.; Sun, X.; Li, D.; Amano, H. Full-duplex light communication with a monolithic multicomponent system. *Light Sci. Appl.* **2018**, *7*, 83.

(9) Pearton, S.; Zolper, J.; Shul, R.; Ren, F. GaN: Processing, defects, and devices. *J. Appl. Phys.* **1999**, *86*, 1−78.

(10) Albrecht, M.; Weyher, J.; Lucznik, B.; Grzegory, I.; Porowski, S. Nonradiative recombination at threading dislocations in n-type GaN: Studied by cathodoluminescence and defect selective etching. *Appl. Phys. Lett.* **2008**, *92*, 231909.

(11) Chernyakov, A.; Sobolev, M.; Ratnikov, V.; Shmidt, N.; Yakimov, E. Nonradiative recombination dynamics in InGaN/GaN LED defect system. *Superlattices Microstruct.* **2009**, *45*, 301−307.

(12) Wang, J.; You, H.; Guo, H.; Xue, J.; Yang, G.; Chen, D.; Liu, B.; Lu, H.; Zhang, R.; Zheng, Y. Do all screw dislocations cause leakage in GaN-based devices? *Appl. Phys. Lett.* **2020**, *116*, 062104.

(13) Hasan, M. R.; Tomal, A. I. In *High-performance GaN-based green LEDs*; ICAEE, 2017.

(14) Matioli, E.; Neufeld, C.; Iza, M.; Cruz, S. C.; Al-Heji, A. A.; Chen, X.; Farrell, R. M.; Keller, S.; Denbaars, S.; Mishra, U.; et al. High internal and external quantum efficiency InGaN/GaN solar cells. *Appl. Phys. Lett.* **2011**, *98*, 132117.

(15) Lu, J.; Zhong, Y.; Zhao, S. Intrinsic excitation-dependent room-temperature internal quantum efficiency of AlGaN nanowires with varying Al contents. *J. Vac. Sci. Technol. B* **2021**, *39*, 022803.

(16) Yamada, Y.; Iwamura, K.; Kuronaka, T.; Shinomura, N.; Okagawa, H.; et al. Internal Quantum Efficiency of Nitride-based Light-Emitting Diodes. *J. light vis. environ.* **2008**, *32*, 191−195.

(17) Lee, I.-H.; Jang, L.-W.; Polyakov, A. Y. Performance enhancement of GaN-based light emitting diodes by the interaction with localized surface plasmons. *Nano Energy* **2015**, *13*, 140−173.

(18) Li, D.; Jiang, K.; Sun, X.; Guo, C. AlGaN photonics: recent advances in materials and ultraviolet devices. *Adv. Opt. Photonics* **2018**, *10*, 43−110.

(19) Shin, H. W.; Son, K. R.; Kim, T. G. Localized surface plasmon-enhanced light emission using platinum nanorings in deep ultraviolet-emitting AlGaN quantum wells. *Opt. Lett.* **2016**, *41*, 88−91.

(20) Hirayama, H.; Fujikawa, S.; Kamata, N. Recent progress in AlGaN-based deep-UV LEDs. *Electron Commun. Jpn.* **2015**, *98*, 1−8.

(21) Zhang, J.; Gao, Y.; Zhou, L.; Gil, Y.-U.; Kim, K.-M. In *Transparent deep ultraviolet light-emitting diodes with a p-type AlN ohmic contact layer, Light-Emitting Devices, Materials, and Applications*; SPIE, 2019; p 1094002.

(22) Bai, J.; Wang, T.; Parbrook, P.; Lee, K.; Cullis, A. A study of dislocations in AlN and GaN films grown on sapphire substrates. *J. Cryst. Growth* **2005**, *282*, 290−296.

(23) Bennett, S. Dislocations and their reduction in GaN. *Mater. Sci. Technol.* **2010**, *26*, 1017−1028.

(24) Yakimov, E. B.; Polyakov, A. Y.; Lee, I.-H.; Pearton, S. J. Recombination properties of dislocations in GaN. *J. Appl. Phys.* **2018**, *123*, 161543.

(25) He, C.; Zhao, W.; Zhang, K.; He, L.; Wu, H.; Liu, N.; Zhang, S.; Liu, X.; Chen, Z. High-quality GaN epilayers achieved by facet-controlled epitaxial lateral overgrowth on sputtered AlN/PSS templates. *ACS Appl. Mater. Interfaces* **2017**, *9*, 43386−43392.

(26) Shin, H.-Y.; Kwon, S.; Chang, Y.; Cho, M.; Park, K. Reducing dislocation density in GaN films using a cone-shaped patterned sapphire substrate. *J. Cryst. Growth* **2009**, *311*, 4167−4170.

(27) Hautakangas, S.; Oila, J.; Alatalo, M.; Saarinen, K.; Liszkay, L.; Seghier, D.; Gislason, H. Vacancy defects as compensating centers in Mg-doped GaN. *Phys. Rev. Lett.* **2003**, *90*, 137402.

(28) Laaksonen, K.; Ganchenkova, M. G.; Nieminen, R. M. Vacancies in wurtzite GaN and AlN. *J. Phys.: Condens. Matter* **2009**, *21*, 015803.

(29) Stampfl, C.; Van de Walle, C. Theoretical investigation of native defects, impurities, and complexes in aluminum nitride. *Phys. Rev. B* **2002**, *65*, 155212.

(30) Van de Walle, C. G.; Neugebauer, J. First-principles calculations for defects and impurities: Applications to III-nitrides. *J. Appl. Phys.* **2004**, *95*, 3851−3879.

(31) Stampfl, C.; Van de Walle, C. G. Doping of Al x Ga 1− x N. *Appl. Phys. Lett.* **1998**, *72*, 459−461.

(32) Van de Walle, C. G.; Stampfl, C.; Neugebauer, J. Theory of doping and defects in III−V nitrides. *Appl. Phys. Lett.* **1998**, *189*, 505−510.

(33) Yan, Q.; Janotti, A.; Scheffler, M.; Van de Walle, C. G. Origins of optical absorption and emission lines in AlN. *Appl. Phys. Lett.* **2014**, *105*, 111104.
(34) Neugebauer, J.; Van de Walle, C. G. Gallium vacancies and the yellow luminescence in GaN. *Appl. Phys. Lett.* **1996**, *69*, 503−505.
(35) Sedhain, A.; Du, L.; Edgar, J. H.; Lin, J.; Jiang, H. The origin of 2.78 eV emission and yellow coloration in bulk AlN substrates. *Appl. Phys. Lett.* **2009**, *95*, 262104.
(36) Kresse, G.; Furthmüller, J. Efficient iterative schemes for ab initio total-energy calculations using a plane-wave basis set. *Phys. Rev. B* **1996**, *54*, 11169.
(37) Kresse, G.; Joubert, D. From ultrasoft pseudopotentials to the projector augmented-wave method. *Phys. Rev. b* **1999**, *59*, 1758.
(38) Perdew, J. P.; Burke, K.; Ernzerhof, M. Generalized gradient approximation made simple. *Phys. Rev. Lett.* **1996**, *77*, 3865.
(39) Zheng, Q.; Chu, W.; Zhao, C.; Zhang, L.; Guo, H.; Wang, Y.; Jiang, X.; Zhao, J. Ab initio nonadiabatic molecular dynamics investigations on the excited carriers in condensed matter systems. *Wiley Interdiscip. Rev. Comput. Mol. Sci.* **2019**, *9*, No. e1411.
(40) Jaeger, H. M.; Fischer, S.; Prezhdo, O. V. Decoherence-induced surface hopping. *J. Chem. Phys.* **2012**, *137*, 22A545.
(41) Liu, J.; Neukirch, A. J.; Prezhdo, O. V. Non-radiative electron−hole recombination in silicon clusters: ab initio non-adiabatic molecular dynamics. *J. Chem. Phys. C* **2014**, *118*, 20702−20709.
(42) Chu, W.; Saidi, W. A.; Zheng, Q.; Xie, Y.; Lan, Z.; Prezhdo, O. V.; Petek, H.; Zhao, J. Ultrafast dynamics of photongenerated holes at a CH3OH/TiO2 rutile interface. *J. Am. Chem. Soc.* **2016**, *138*, 13740−13749.
(43) Wei, Y.; Long, R. Grain boundaries are benign and suppress nonradiative electron−hole recombination in monolayer black phosphorus: a time-domain ab initio study. *J. Phys. Chem. Lett.* **2018**, *9*, 3856−3862.
(44) Zhang, L.; Chu, W.; Zheng, Q.; Benderskii, A. V.; Prezhdo, O. V.; Zhao, J. Suppression of electron−hole recombination by intrinsic defects in 2D monoelemental material. *J. Phys. Chem. Lett.* **2019**, *10*, 6151−6158.
(45) Chu, W.; Zheng, Q.; Prezhdo, O. V.; Zhao, J.; Saidi, W. A. Low-frequency lattice phonons in halide perovskites explain high defect tolerance toward electron-hole recombination. *Sci. Adv.* **2020**, *6*, No. eaaw7453.
(46) Zhang, P.; Hou, Z.; Jiang, L.; Yang, J.; Saidi, W. A.; Prezhdo, O. V.; Li, W. Weak Anharmonicity Rationalizes the Temperature-Driven Acceleration of Nonradiative Dynamics in Cu2ZnSnS4 Photoabsorbers. *ACS Appl. Mater. Interfaces* **2021**, *13*, 61365−61373.
(47) Zhou, Z.; Liu, J.; Long, R.; Li, L.; Guo, L.; Prezhdo, O. V. Control of charge carriers trapping and relaxation in hematite by oxygen vacancy charge: ab initio non-adiabatic molecular dynamics. *J. Am. Chem. Soc.* **2017**, *139*, 6707−6717.
(48) Akimov, A. V.; Prezhdo, O. V. Advanced capabilities of the PYXAID program: integration schemes, decoherence effects, multi-excitonic states, and field-matter interaction. *J. Chem. Theory Comput.* **2014**, *10*, 789−804.
(49) Pal, S.; Trivedi, D. J.; Akimov, A. V.; Aradi, B.; Frauenheim, T.; Prezhdo, O. V. Nonadiabatic molecular dynamics for thousand atom systems: a tight-binding approach toward PYXAID. *J. Chem. Theory Comput.* **2016**, *12*, 1436−1448.
(50) Chu, W.; Prezhdo, O. V. Concentric approximation for fast and accurate numerical evaluation of nonadiabatic coupling with projector augmented-wave pseudopotentials. *J. Phys. Chem. Lett.* **2021**, *12*, 3082−3089.
(51) Chu, W.; Zheng, Q.; Akimov, A. V.; Zhao, J.; Saidi, W. A.; Prezhdo, O. V. Accurate computation of nonadiabatic coupling with projector augmented-wave pseudopotentials. *J. Phys. Chem. Lett.* **2020**, *11*, 10073−10080.
(52) Wang, B.; Chu, W.; Tkatchenko, A.; Prezhdo, O. V. Interpolating nonadiabatic molecular dynamics Hamiltonian with artificial neural networks. *J. Phys. Chem. Lett.* **2021**, *12*, 6070−6077.
(53) Bungaro, C.; Rapcewicz, K.; Bernholc, J. Ab initio phonon dispersions of wurtzite AlN, GaN, and InN. *Phys. Rev. B* **2000**, *61*, 6720.
(54) Martin, G.; Strite, S.; Botchkarev, A.; Agarwal, A.; Rockett, A.; Morkoc, H.; Lambrecht, W.; Segall, B. Valence-band discontinuity between GaN and AlN measured by x-ray photoemission spectroscopy. *Appl. Phys. Lett.* **1994**, *65*, 610−612.
(55) Cheng, C.; Prezhdo, O. V.; Long, R.; Fang, W.-H. Photolysis versus photothermolysis of N2O on a semiconductor surface revealed by nonadiabatic molecular dynamics. *J. Am. Chem. Soc.* **2023**, *145*, 476−486.
(56) Wang, H.; Zhou, Z.; Long, R.; Prezhdo, O. V. Passivation of Hematite by a Semiconducting Overlayer Reduces Charge Recombination: An Insight from Nonadiabatic Molecular Dynamics. *J. Phys. Chem. Lett.* **2023**, *14*, 879−887.
(57) Jia, Y.; Shi, Z.; Hou, W.; Zang, H.; Jiang, K.; Chen, Y.; Zhang, S.; Qi, Z.; Wu, T.; Sun, X.; et al. Elimination of the internal electrostatic field in two-dimensional GaN-based semiconductors. *NPJ. 2D Mater. Appl.* **2020**, *4*, 31.
(58) Davydov, V. Y.; Kitaev, Y. E.; Goncharuk, I.; Smirnov, A.; Graul, J.; Semchinova, O.; Uffmann, D.; Smirnov, M.; Mirgorodsky, A.; Evarestov, R. Phonon dispersion and Raman scattering in hexagonal GaN and AlN. *Phys. Rev. B* **1998**, *58*, 12899.
(59) Gao, Y.; Sun, D.; Jiang, X.; Zhao, J. Point defects in group III nitrides: A comparative first-principles study. *J. Appl. Phys.* **2019**, *125*, 215705.
(60) Mattila, T.; Nieminen, R. M. Point-defect complexes and broadband luminescence in GaN and AlN. *Phys. Rev. B* **1997**, *55*, 9571.
(61) Tuomisto, F.; Mäki, J.-M.; Rauch, C.; Makkonen, I. On the formation of vacancy defects in III-nitride semiconductors. *J. Cryst. Growth* **2012**, *350*, 93−97.
(62) Johnson, N. M.; Nurmikko, A. V.; DenBaars, S. P. Blue diode lasers. *Phys. Today* **2000**, *53*, 31−36.
(63) Nakamura, S.; Fasol, G. *The blue laser diode: GaN based light emitters and lasers*; Springer, 2013.
(64) Shatalov, M.; Yang, J.; Sun, W.; Kennedy, R.; Gaska, R.; Liu, K.; Shur, M.; Tamulaitis, G. Efficiency of light emission in high aluminum content AlGaN quantum wells. *J. Appl. Phys.* **2009**, *105*, 073103.

https://doi.org/10.1021/acs.jpclett.3c01515
J. Phys. Chem. Lett. 2023, 14, 6719−6725